Mühendislik Bilimleri ve Tasarım Dergisi
13(3), 932-943, 2025
e-ISSN: 1308-6693

Journal of Engineering Sciences and Design
DOI: 10.21923/jesd.1676129

Araştırma Makalesi Research Article

INVESTIGATION OF RADIATION SHIELDING PROPERTIES OF EIGHT WOOD SPECIES WITH XCOM PROGRAM AND EXPERIMENTAL DATA

Yasemin ŞİMŞEK TÜRKER*, Şemsettin KILINÇARSLAN[1]

[1]Suleyman Demirel University, Faculty of Engineering and Nature, Department of Civil Engineering, Isparta, Türkiye

Keywords

Building Material, Wood Material, Radiation, XCOM.

Abstract

In this study, radiation shielding properties of 8 different wood species (T1–T8) were investigated experimentally and theoretically using the XCOM program. The densities and elemental compositions of the samples were determined by EDAX analysis, and a NaI (Tl) detector was used in gamma spectroscopy experiments performed at energy levels of 662 keV, 1173 keV and 1332 keV. Strong correlations were observed between the linear attenuation coefficient (LAC) obtained from the experimental data and the density; this relationship was particularly evident at 662 keV (R^2 = 0.9195, slope = 0.0792). The highest mass attenuation coefficient (MAC) values were determined as ~0.085 at 662 keV in samples T3, T4 and T5. On the other hand, the lowest MAC values were observed in sample T1 (between ~0.045–0.060). The half-value layer (HVL) values increased with energy; Sample T1 had the highest HVL at all energies, reaching approximately 125 mm at 1173 keV. HVL values for species such as T4 and T5 remained in the range of 10–30 mm. Similarly, the tenth value layer (TVL) and mean free path (MFP) values were measured at the highest levels for T1; at 1332 keV, TVL reached approximately 420 mm and MFP reached 180 mm. These values were lower for other wood species. The theoretical MAC values obtained with the XCOM program were found to be in very good agreement with the experimental data (R^2 > 0.98). These results demonstrated that high-density wood species provide more effective attenuation against low-energy gamma photons and that the XCOM program is a reliable tool for the radiation protection analysis of wood materials.

XCOM PROGRAMI VE DENEYSEL VERILERLE SEKIZ AĞAÇ TÜRÜNÜN RADYASYON TUTUCULUK ÖZELLIKLERININ ARAŞTIRILMASI

Anahtar Kelimeler

Yapı Malzemesi, Ahşap Malzeme, Radyasyon, XCOM.

Öz

Bu çalışmada, 8 farklı ağaç türünün (T1–T8) radyasyon zayıflatma özellikleri deneysel olarak ve XCOM programı kullanılarak teorik olarak incelenmiştir. Numunelerin yoğunlukları ile elementel bileşimleri EDAX analizi ile belirlenmiş, 662 keV, 1173 keV ve 1332 keV enerji seviyelerinde gerçekleştirilen gamma spektroskopisi deneylerinde NaI (Tl) dedektörü kullanılmıştır. Deneysel verilerden elde edilen lineer zayıflama katsayısı (LAC) ile yoğunluk arasında güçlü korelasyonlar gözlenmiş, özellikle 662 keV'de bu ilişki oldukça belirgindir (R^2=0.9195, eğim = 0.0792). En yüksek kütle soğurma katsayısı (MAC) değerleri 662 keV enerjisinde T3, T4 ve T5 numunelerinde ~0.085 olarak belirlenmiştir. Buna karşılık en düşük MAC değerleri T1 numunesinde (~0.045–0.060 arası) gözlenmiştir. Yarı değer tabakası (HVL) değerleri enerjiyle birlikte artış göstermiş; T1 numunesi tüm enerjilerde en yüksek HVL'ye sahip olup, 1173 keV'de yaklaşık 125 mm'ye ulaşmıştır. T4 ve T5 gibi türlerde HVL değerleri 10–30 mm aralığında kalmıştır. Onda bir değer tabakası (TVL) ve ortalama serbest yol (MFP) değerleri de benzer şekilde T1 için en yüksek seviyelerde ölçülmüş; 1332 keV'de TVL yaklaşık 420 mm, MFP ise 180 mm'ye ulaşmıştır. Diğer ağaç türlerinde bu değerler daha düşük kalmıştır. XCOM programı ile elde edilen teorik MAC değerleri ile deneysel veriler arasında oldukça yüksek uyum bulunmuştur (R^2>0.98). Bu sonuçlar, yüksek yoğunluklu ağaç türlerinin düşük enerjili gamma fotonlarına karşı daha etkin zayıflatma sağladığını ve XCOM programının ahşap malzemelerin radyasyon koruma analizinde güvenilir bir araç olduğunu ortaya koymuştur.

* İlgili yazar / Corresponding author: yaseminturker@sdu.edu.tr, +90-246-211-1267

Alıntı / Cite

Şimşek Türker, Y., Kılınçarslan, Ş. (2025). Investigation of Radiation Shielding Properties of Eight Wood Species with XCOM Program and Experimental Data, Journal of Engineering Sciences and Design, 13(3), 932-943.

Yazar Kimliği / Author ID (ORCID Number)	Makale Süreci / Article Process	
Y. Şimşek Türker, 0000-0002-3080-0215	**Başvuru Tarihi / Submission Date**	14.03.2025
Ş. Kılınçarslan, 0000-0001-8253-9357	**Revizyon Tarihi / Revision Date**	03.08.2025
	Kabul Tarihi / Accepted Date	25.08.2025
	Yayım Tarihi / Published Date	30.09.2025

INVESTIGATION OF RADIATION SHIELDING PROPERTIES OF EIGHT WOOD SPECIES WITH XCOM PROGRAM AND EXPERIMENTAL DATA

Yasemin ŞİMŞEK TÜRKER†, Şemsettin KILINÇARSLAN
Suleyman Demirel University

Highlights

- A strong linear relationship between intensity and linear attenuation coefficient was observed for 662 keV low-energy photons.
- The photon attenuation capacity decreases as the energy level increases.
- Wood samples T3, T4, and T5 showed the highest photon attenuation at 662 keV.
- High agreement was found between experimental and theoretical data.

Purpose and Scope

The purpose of this paper is to investigate the attenuation performance of selected wood species against gamma radiation at different energy levels, both experimentally and theoretically. The research aims to analyze the relationship between photon energy, wood density, and the material's ability to attenuate gamma radiation, providing valuable insights for material selection in radiation shielding applications.

Design/methodology/approach

The objectives of the research are achieved through experimental and theoretical methods. Gamma radiation attenuation measurements are conducted on selected wood species at three different energy levels to determine the linear attenuation coefficient and other related parameters. Theoretical data are compared with experimental results using the XCOM software for validation. The study takes a comparative approach, analyzing the relationship between wood density, energy levels, and photon attenuation. The theoretical scope involves applying principles of radiation physics, while the experimental approach focuses on real-world wood samples and their potential use in radiation shielding.

Findings

The findings of the study reveal that wood species exhibit varying attenuation performances against gamma radiation at different energy levels. A strong linear relationship was observed between the intensity and linear attenuation coefficient for low-energy photons (662 keV), indicating that these photons interact more with the wood's atomic structure. The attenuation capacity decreases as the energy level increases, with high-energy photons (1332 keV) penetrating deeper into the material. Wood samples T3, T4, and T5 showed the highest photon attenuation, particularly at 662 keV, while sample T1 demonstrated the lowest attenuation and highest half-value and tenth-value thickness, indicating poor performance in photon attenuation. The experimental results were in high agreement with theoretical data, reinforcing the validity of the measurements.

Originality

This paper introduces a comprehensive analysis of gamma radiation attenuation in various wood species across different energy levels, highlighting the significant role of wood density and structure in radiation shielding. The study provides valuable insights into the specific attenuation behaviors of different wood types, particularly for low-energy photons, which have not been extensively explored in previous research. The findings are valuable for researchers and professionals in the fields of materials science, radiation protection, and environmental engineering, offering practical guidance for selecting appropriate biomaterials for radiation shielding applications.

† Corresponding author: yaseminturker@sdu.edu.tr, +90-246-211-1267

1. Introduction

High-energy ionizing radiations, which include both indirectly ionizing types such as photons and neutrons, as well as directly ionizing types like electrons, protons, and alpha particles, are extensively utilized in various radiation technologies. These applications span various sectors, including energy production, nuclear research, electricity generation in nuclear power plants, radiotherapy, medical diagnostic and therapeutic techniques, agriculture, the oil industry, space technology, environmental monitoring, archaeological research, and many other industrial domains (Shamshad et al., 2017). Despite their widespread use, exposure to ionizing radiation poses significant risks to human health due to the high energy carried by photons. Numerous studies have indicated that improper or unsafe handling of ionizing radiation technologies can result in biological damage to living tissues, potentially leading to severe health issues such as cancer and even death. Ionizing radiation possesses enough energy to dislodge electrons from atoms, which can result in substantial harm if appropriate safety protocols are not followed (Sadetzki and Mandelzweig, 2009; Vano, 2011; Mettler, 2012; Rachniyom et al., 2018; Waly and Bourham, 2015). To safeguard individuals from various forms of radiation, protective shielding materials are employed to absorb incoming photons, thereby reducing the potential risks associated with radiation exposure (Kurudirek, 2017). The selection of suitable materials for shielding depends on the type of radiation involved and the specific application. The characteristics of radiation shielding materials differ based on the type of radiation that needs to be mitigated, the energy levels of the photons, and the context in which they are used. For instance, the material chosen to shield against X-rays in a medical facility will differ significantly from the materials used for constructing the walls of a nuclear plant. Regardless of the specific application, all shielding materials are designed with the same objective: to absorb the maximum possible amount of radiation while ensuring practical usability (Al-Hadeethi and Sayyed, 2020). In nuclear reactors, the primary radiation types that require shielding include neutrons and gamma rays generated within the reactor core, as well as secondary gamma rays produced from the interactions of neutrons with external materials in the reactor (Singh et al., 2008). Traditionally, radiation shielding in nuclear reactors has involved the use of a steel-clad thermal shield to protect the reactor walls, coupled with a concrete biological shield to protect personnel from radiation exposure (Akiyama et al., 1989). Gamma rays, which are a form of ionizing radiation emitted during nuclear decay, possess extremely high photon energy (Kurudirek, 2017). The ability of a material to attenuate gamma radiation is influenced by its physical and chemical properties. Effective shielding materials typically have high mass density and a large effective atomic number, which allows them to reduce photon intensity through processes such as scattering or photoemission (Singh et al., 2008; Mann and Sidhu, 2012; Singh and Badiger, 2014; Agar et al., 2019; Sharma et al., 2019).

Various international radiation organizations have proposed guidelines to reduce the risks of radiation exposure to human tissues and organs. Among the most widely recognized principles for radiation protection are Medical Internal Radiation Dose and As Low as Reasonably Achievable (ALARA). ALARA is a well-established principle of radiation safety that focuses on minimizing radiation doses by considering three key factors: distance, time, and shielding. Specifically, reducing the duration of exposure helps lower the radiation dose, increasing the distance between the individual (whether a worker or patient) and the radiation source diminishes exposure, and utilizing appropriate shielding materials, such as lead or lead-equivalent materials, further reduces radiation risks (Shavers et al., 2004; Sodhi et al., 2015; D'Auria et al., 2017). A significant amount of research has been dedicated to the design and development of new radiation shielding materials, along with more precise computational methods for analyzing radiation interactions (Abouhaswa et al., 2019; Al-Buriahi and Tonguc, 2019; Ersundu et al., 2019; Sayyed et al., 2020). Consequently, the literature includes various studies exploring alternative materials, such as building materials, bricks, concrete, polymers, steel, resins, composites, ceramics, and alloys, to assess their potential for radiation shielding applications (Sharma et al., 2012; Bootjomchai et al., 2012; Kaewjaeng et al., 2012; Singh et al., 2014; El-Khayatt et al., 2014; Waly and Bourham, 2015; Sayyed et al., 2018; Shams et al., 2018; Cherkashina and Pavlenko, 2018; Al-Buriahi and Rammah, 2019b; Cherkashina et al., 2019; Al-Buriahi and Tonguc, 2020). However, while many of these studies have focused on conventional materials such as concrete, leaded glass, and polymer composites, there remains a noticeable gap in the literature regarding the radiation attenuation properties of natural and sustainable materials particularly wood. Despite its widespread use in architecture and design, wood has been relatively underexplored in the context of radiation shielding. Most existing wood studies are limited in sample diversity or do not compare results against theoretical data for validation.

This study addresses this gap by experimentally investigating the gamma radiation shielding capabilities of sixteen different tree species with varying densities. The research not only evaluates experimental parameters such as the linear attenuation coefficient (μ), mass attenuation coefficient (μ/ρ), half-value layer (HVL), tenth value layer (TVL), and mean free path (MFP), but also compares these results with theoretical values obtained from the XCOM program. This dual approach helps to validate the experimental findings and offers insights into the viability of wood as a radiation shielding material, especially for applications requiring lightweight, biodegradable, or non-toxic alternatives.

2. Material and Method

After the wood samples were obtained from different regions, they were processed in an oven at 100 ◦C for several days to dry. These samples were weighed every day, and their weight fluctuations were tracked until the rate of weight change dropped below 0.15% per day. Then, these samples were considered stable since the moisture content changed with time. The 8 samples studied are Balsa, Ayous, Poplar, Jupiner, Chestnut, Oak, Service, and Paddock. The codes of the samples are given as T1, T2, T3, T4, T5, T6, T7 and T8, respectively.

2.1. Physical properties of the wood

Rectangular shapes were applied to the samples. For every slice, the volume of the samples was calculated by multiplying the appropriate thickness, breadth, and length. Each sample's length, width, and thickness were measured, and the density of the wood was computed using the formula below.

$$\rho = m/v \qquad (1)$$

Where ρ is density, v is volume and m is the mass of the wood samples.

2.2. Elemental analysis (EDAX)

In this study, the EDAX device located at the YETEM Research Center of Süleyman Demirel University was used to perform elemental analysis of wood materials. Samples of 5x5x10 mm dimensions were prepared for the experiment. The analysis of the C, O, Mg, Na, Mg, Al, Si, K, Ca, Ba, Mn, Fe and Zn elements of the samples was performed. The EDAX elemental analysis device used in the study is given in Figure 1.

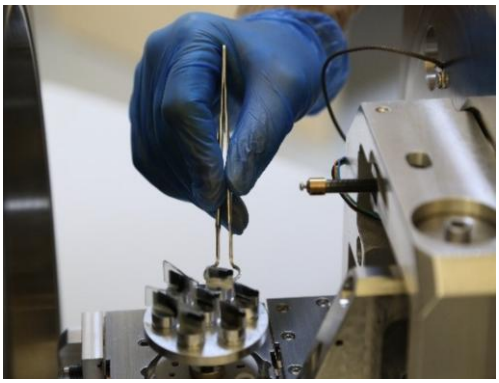

Figure 1. EDAX elemental analysis device

The elemental analysis results obtained because of the experiment were used to obtain theoretical findings.

2.3. Experimental Radiation Measurements

In the Gamma Spectroscopy Laboratory, radiation shielding experiments were carried out. The released gamma rays contact with the NaI (TI) detector in a gamma spectroscopy system to separate them according to their energy. Radiation absorption coefficients were assessed using the Na (TI) scintillation detector in the radiation shielding experimental setup. The two main parts of a scintillation detector are the scintillator, which is a sparkling material, and the photomultiplier tube, which contains the photocathode, electrode, electron multipliers, and anode. After entering the scintillator, the gamma-ray interacts with specific solid, liquid, or gaseous substances called scintillation phosphors to produce excitation and ionization. When there is not enough energy to extract gamma-ray-excited electrons from their surroundings, they return to their initial state and emit light. The light that is released is collected by photomultiplier tubes, which then convert it into a voltage pulse. The amplitude of this pulse is determined by the radiation's energy. Energy separation and counting are more applications for these detectors. The signals produced by gamma radiation in the NaI (TI) detector are enhanced and reshaped to provide the appropriate energy separation with the help of an amplifier. The signal from the amplifier is received by the Multi-Channel Analyzer (MCC), which converts it into digital form using its 16384 channels, each of which represents an energy. The digitally altered data from the analyzer appears on the screen as a spectrum. The high-voltage unit powers the system (Akkurt et al., 2010; Akkurt et al., 2012; Akkurt et al., 2015). The sample will be positioned equally between the source and the detector throughout the trials, as shown in Figure 2. In this study, the distance between the gamma source and the detector was kept constant, and all measurements were

performed according to this fixed geometry. This distance was set at approximately 20 cm, ensuring proper alignment along the source-sample-detector line. This aimed to prevent potential variations in dose due to distance that could affect the measurements. Furthermore, the same source activity was used in each measurement.

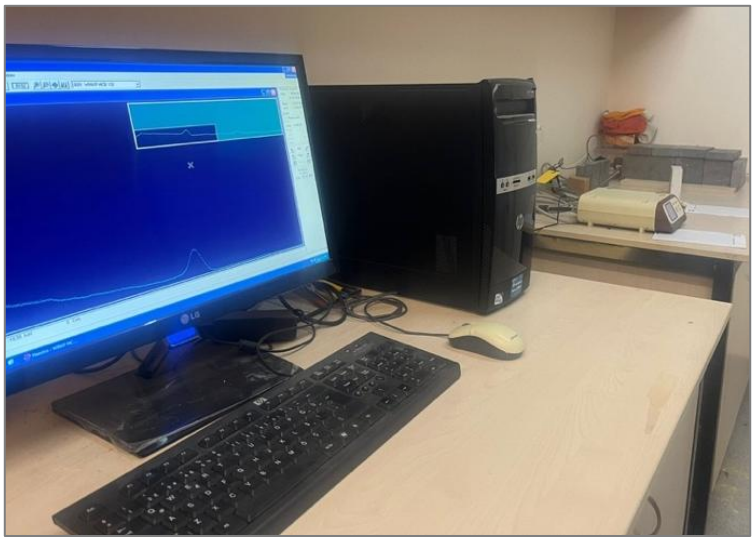

Figure 2. Schematic and real images of the detector and electronic devices that make up the gamma spectroscopy system

The same reference measurement was used to measure each concrete. The samples were then placed between the source and the detector. Concrete radiation absorption coefficients were measured at 662 keV, 1173 keV, and 1332 keV energy using ^{137}Cs and ^{60}Co radioactive sources.

The linear attenuation coefficient (LAC) is a key parameter used to characterize the effectiveness of shielding materials in reducing incident radiation. It considers various interactions of ionizing radiation with matter, such as the photoelectric effect, Compton scattering, and Rayleigh scattering (Mahmoud et al., 2019; Mahmoud and Rammah, 2020). The equation below demonstrates the exponential calculation of the linear attenuation coefficient, following the Beer-Lambert law:

$$I = I_0 \exp(-\mu.t) \quad (2)$$

Where I denote the ionizing photons that have been attenuated, I_0 refers to the ionizing photons that remain non-attenuated, μ represents the linear attenuation coefficient (in cm^{-1}), and t indicates the thickness of the material (in cm).

One important photon shielding parameter is the MAC, which provides insight into the number of photons that are scattered or absorbed by the interacting material. The MAC, which describes the ability of ionizing photons to pass through a particular material (Almatari et al., 2019), can be mathematically represented by the following equation:

$$\mu = \mu\ (2)\ m\ /\rho \quad (3)$$

μm (cm^2/g) represents the mass attenuation coefficient, while ρ (g/cm^3) is the material's density. The mean free path (MFP) refers to the average distance an energetic photon travels before undergoing a series of interactions with matter (Kumar et al., 2020). The MFP (in cm) can be derived from the calculated LAC value and is mathematically expressed as follows:

$$MFP = 1/\mu \quad (4)$$

Other significant radiation shielding parameters of a material are the HVL and TVL, which are regularly used to evaluate the shielding effectiveness of various materials. The term HVL refers to the thickness of the shielding material that is sufficient to reduce the radiation intensity from the source by 50%, through either scattering or absorption (Waly et al., 2016). The half-value layer (HVL, in cm) is determined using the linear attenuation coefficient (μ) with the following equation:

$$HVL = \ln 2/\mu \quad (5)$$

The tenth (TVL) defines the thickness of the interacting target at which the attenuated intensity is 90% of the narrow photon beam intensity. The TVL (in cm) is related to the linear attenuation coefficient by the following equation:

$$TVL = \ln 10/\mu \quad (6)$$

2.4. Theoretical Radiation Measurements

In this study, 8 different types of wood samples were used. The samples were cut to certain sizes and subjected to EDAX analysis after the surface was cleaned. They were made ready for analysis. The elemental composition of the wood samples was determined by the energy-dispersive X-ray spectroscopy (EDAX) method. EDAX measurements were performed using a specific electron beam and the elemental composition in the samples was determined by analyzing the obtained spectra. As a result of this analysis, the percentage ratios of the elements contained in the samples were obtained. The XCOM program is a software used to calculate the mass attenuation coefficient of different materials. The elemental composition percentages obtained from the EDAX analysis were entered into the program as input data. As seen in Figure 3, the chemical compositions obtained from the EDAX analysis of the wood samples were used.

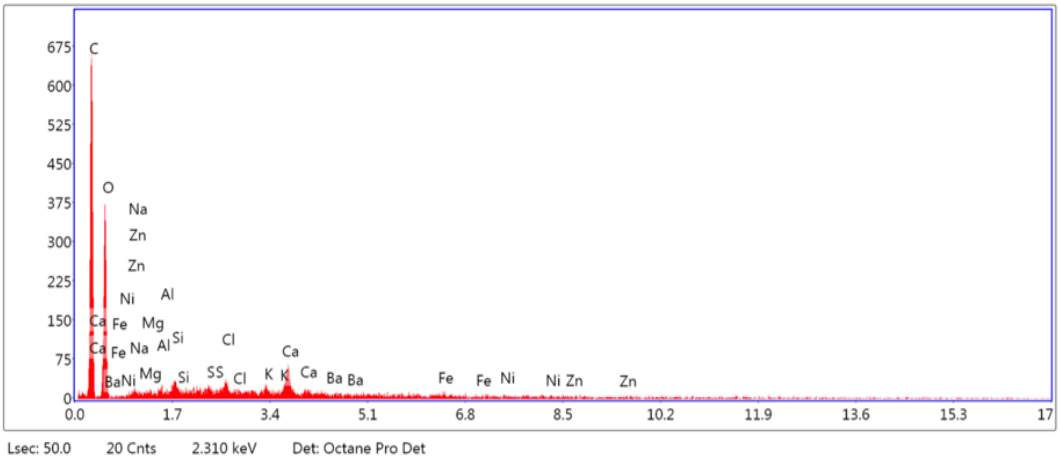

Figure 3. The EDAX spectrum example of a wood sample.

The percentage ratios of the elements found in these compositions, as well as the analysis wavelength or energy, are also defined in the XCOM program. The XCOM program calculates the mass absorption coefficient based on the elemental composition and energy values entered. The program lists the absorption values at different energies and presents the results to the user. The program provides an output containing the mass absorption coefficient values at each energy level according to the entered parameters. These outputs were compared with the experimental results and evaluated. The differences between the values at different energies were analyzed and the accuracy level of the program was evaluated. The results were also shown graphically, and the deviations were interpreted. An example of XCOM theoretical analysis results is given in Figure 4.

```
Z=6     : 0.507249
Z=8     : 0.481252
Z=11    : 0.000000
Z=12    : 0.000900
Z=13    : 0.000100
Z=14    : 0.000400
Z=19    : 0.003200
Z=20    : 0.004300
Z=25    : 0.000400
Z=26    : 0.000700
Z=30    : 0.000400
Z=56    : 0.001100
```

Edge	(required) Photon Energy	Scattering		Photoelectric Absorption	Pair Production		Total Attenuation	
		Coherent	Incoherent		In Nuclear Field	In Electron Field	With Coherent Scattering	Without Coherent Scattering
	MeV	cm²/g	cm²/g	cm²/g	cm²/g	cm²/g	cm²/g	cm²/g
	6.620E-01	1.243E-04	7.705E-02	2.375E-05	0.000E+00	0.000E+00	7.720E-02	7.707E-02
	1.173E+00	3.967E-05	5.874E-02	6.915E-06	6.082E-06	0.000E+00	5.880E-02	5.876E-02
	1.332E+00	3.076E-05	5.502E-02	5.519E-06	3.649E-05	0.000E+00	5.509E-02	5.506E-02

Figure 4. An example of XCOM theoretical analysis results

This methodology was created to evaluate the applicability of the XCOM program for wood materials, and the comparison of the experimental findings with the theoretical calculations was provided.

3. Experimental Results

In this study, the density and radiation retention values of wooden materials were determined experimentally. The linear attenuation coefficient values depending on the obtained density values are given in Figure 5.

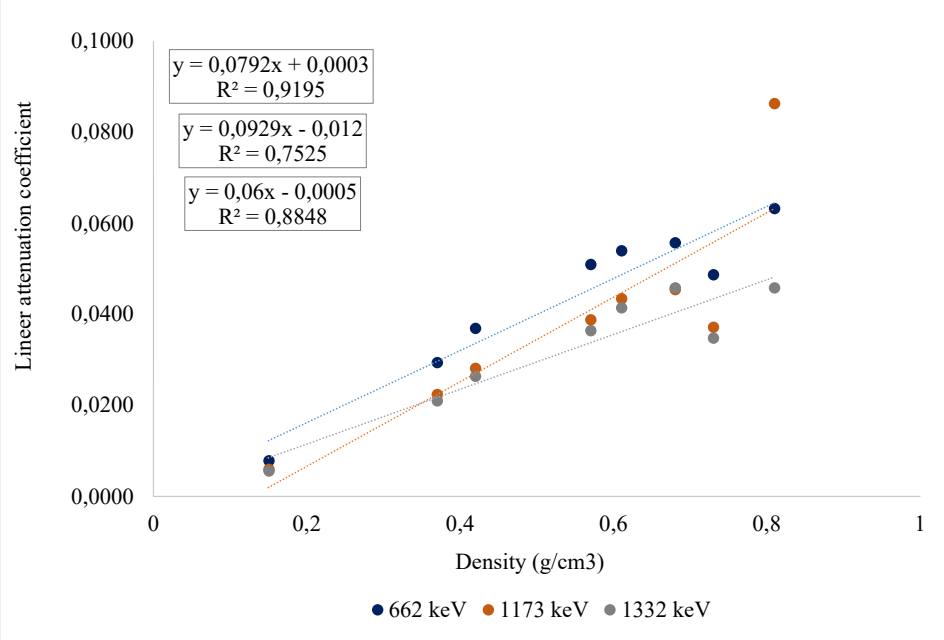

Figure 5. Density-linear attenuation coefficient chart

In Figure 5, the relationship between the linear attenuation coefficient of gamma rays at different energies (662 keV, 1173 keV, and 1332 keV) and the intensity is investigated. As the intensity increases at all energy levels, the linear attenuation coefficient also increases, and this relationship is observed most strongly at 662 keV (R^2 = 0.9195, slope = 0.0792). Although the relationship is weaker for 1173 keV (R^2 = 0.7525), the slope value is the highest at this energy level (0.0929), showing a greater attenuation change with increasing intensity. At the highest energy, 1332 keV, the slope value is the lowest (0.06), and although the R^2 value (0.8848) is high, the attenuation coefficient is less sensitive to the intensity. These results show that lower energy photons are attenuated more in the material and show a stronger linear relationship with density, indicating that this should be taken into consideration, especially in terms of radiation shielding and material selection. The MAC and HVL results obtained by experimentally measuring radiation retention are given in Figure 6 and Figure 7.

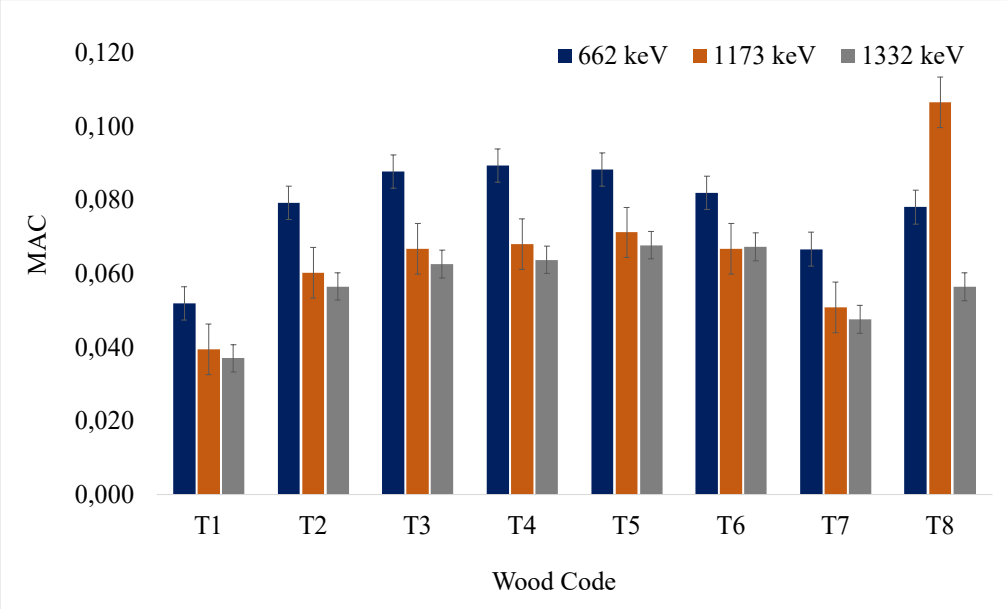

Figure 6. MAC values of woods

In Figure 6, MAC values for different tree species (T1–T8) are compared at three different gamma energies (662 keV, 1173 keV, 1332 keV). In general, the highest MAC values are observed for 662 keV at all three energy levels, indicating that low-energy photons interact more with the material. While the MAC values for 662 keV are at the level of 0.085 in samples T3, T4, and T5, they are around 0.065 for 1173 keV and 0.060 for 1332 keV in the same samples. The lowest MAC values are observed in sample T1, indicating that T1 attenuates photons less due to its lower density or elemental structure.

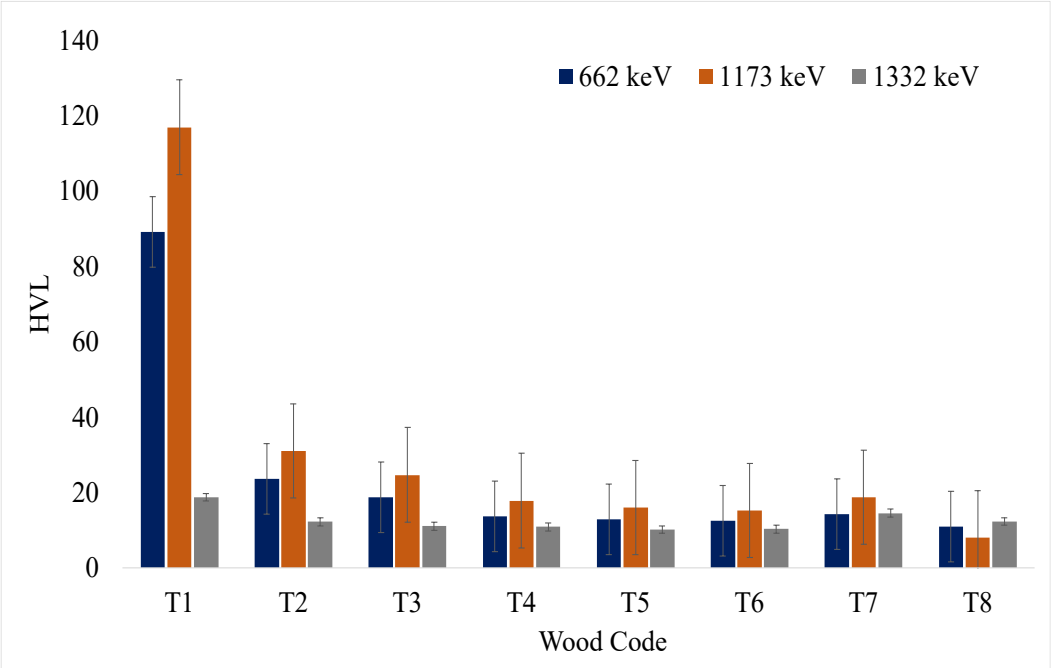

Figure 7. HVL values of woods

HVL values for tree species are presented in Figure 7. HVL values increase as photon energy increases because photons with higher energy penetrate more. The T1 sample has the highest HVL values by far at all energy levels, especially reaching approximately 125 mm at 1173 keV, exhibiting the lowest attenuation property. HVL values are closer to each other in all other tree species, generally ranging between 10 and 30 mm. It is seen that there is an inverse relationship between HVL values and MAC because HVL is lower in samples with high MAC values. In this context, it can be said that samples such as T3, T4, and T5 are more effective in terms of radiation attenuation, while T1 has the weakest performance. These results show that tree species such as T3, T4, and T5 may be more suitable radiation shielding materials against low-energy photons. TVL and MFP results obtained by experimentally measuring radiation retention are given in Figure 8 and Figure 9.

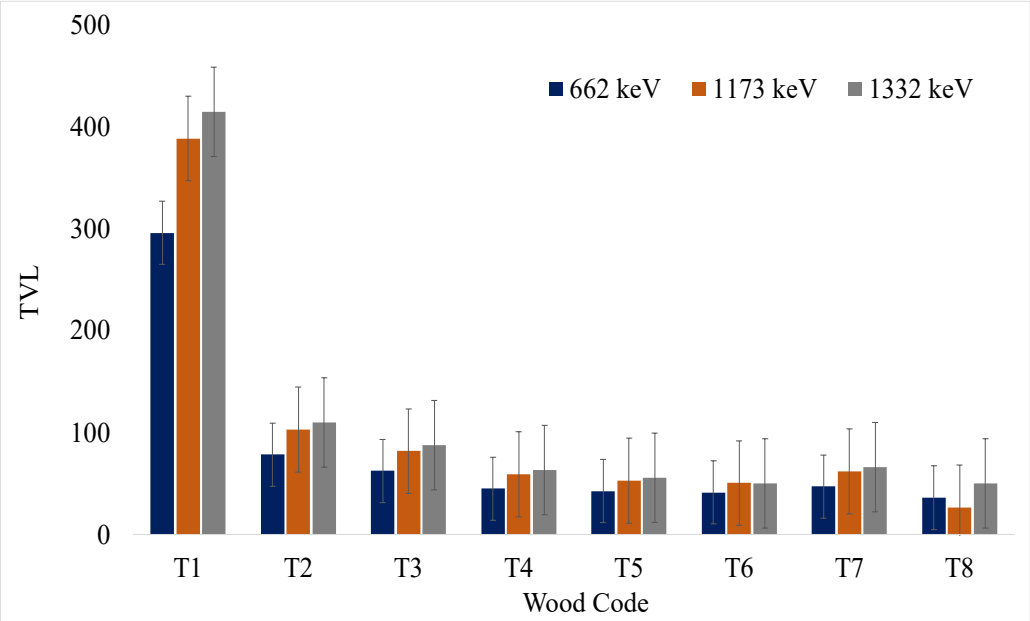

Figure 8. TVL values of woods

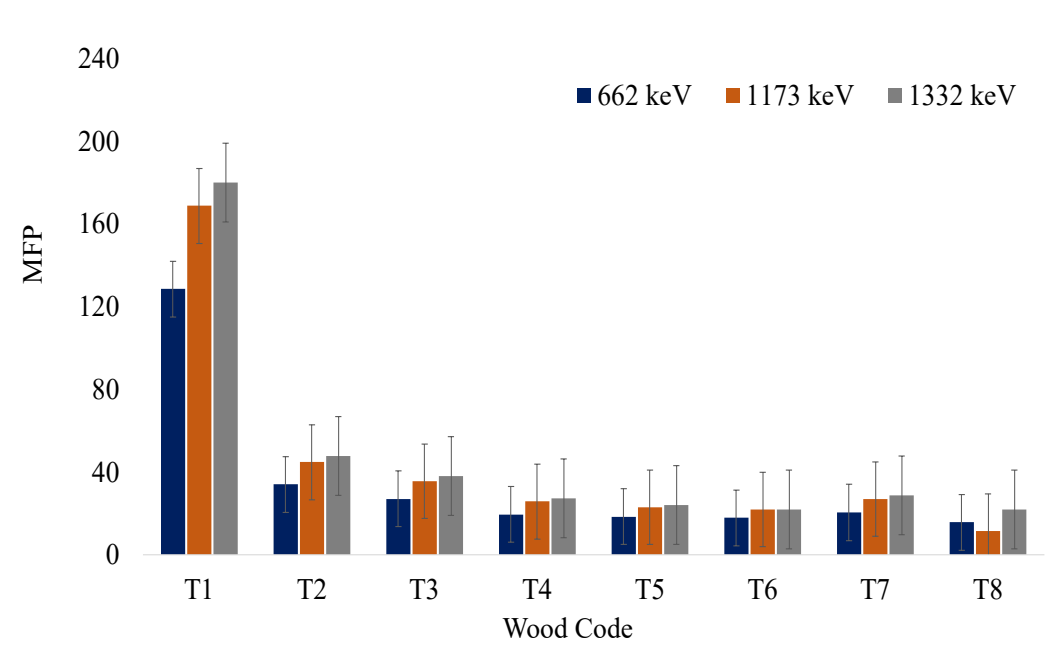

Figure 9. MFP values of woods

Both graphs were prepared to compare the attenuation capacities of different wood species (T1–T8) against gamma rays at three different energy levels (662 keV, 1173 keV, and 1332 keV). TVL (Tenth Value Layer) values are presented in the first graph, and MFP (Mean Free Path) values are presented in the second graph. Both TVL and MFP values provide information about the attenuation efficiency of the material; in this context, lower values indicate higher attenuation capacity. In both graphs, it is seen that T1-coded wood has the highest TVL and MFP values at all energy levels; this situation reveals that T1 has the lowest efficiency in terms of attenuation of gamma rays. Especially for T1, while TVL is approximately 420 units at the 1332 keV energy level, the MFP value approaches 180 units. On the other hand, TVL and MFP values are significantly lower in other wood types such as T4, T5, T6, T7, and vary very little according to the energy level. These wood types generally have higher attenuation performance. In addition, a slight increase in TVL and MFP values is observed in both graphs as the energy level increases, indicating that high-energy photons are attenuated less by the material. As a result, wood types other than T1 show more effective attenuation properties, especially at the energy levels of 662 keV and 1173 keV, and their potential for use as radiation shielding materials is higher structurally. The MAC values obtained with the XCOM program and the experimentally obtained MAC values are compared in Figure 10.

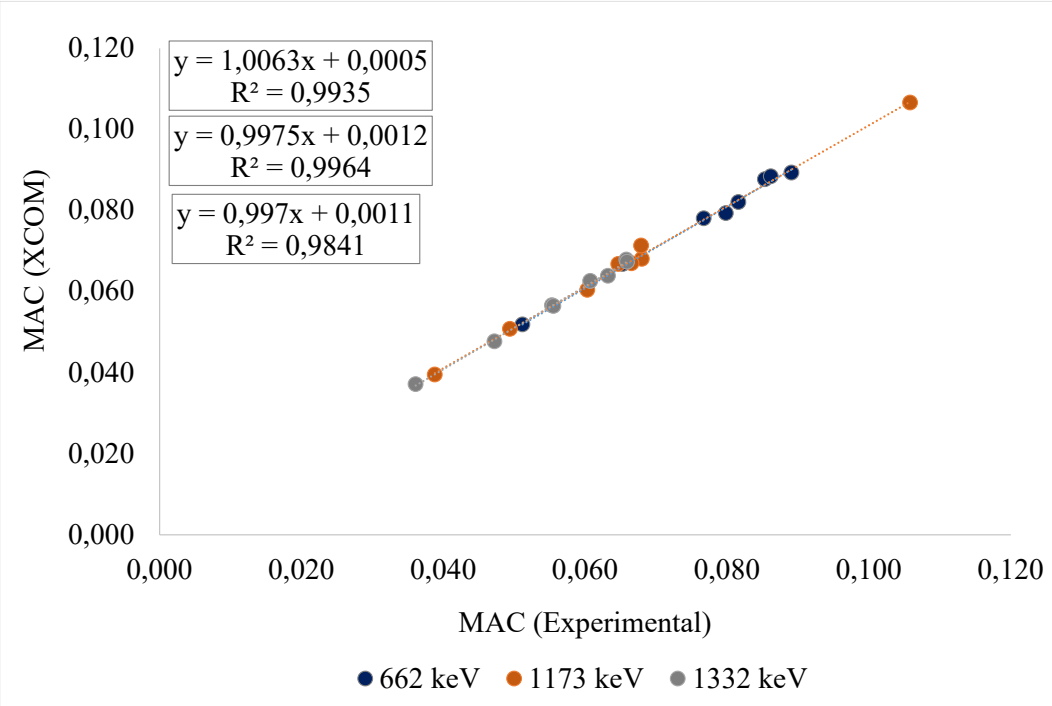

Figure 10. Experimental and XCOM obtained MAC values

In the graph, the relationship between the experimentally obtained mass attenuation coefficient (MAC) values at different energy levels (662 keV, 1173 keV and 1332 keV) and the theoretical XCOM data is examined. Quite high correlation coefficients (R^2>0.98) were obtained between the experimental and theoretical data for all three energy levels. This high agreement shows the reliability of the experimental data and the accuracy of the measurements. The distribution of the data progresses quite close to the theoretical model regardless of the energy level and reveals that the experimental methods give consistent results with the XCOM database. These findings support the validity of the study by showing that the attenuation properties of the wood samples used can be evaluated both experimentally and theoretically in a similar way. Of the wood species included in our study, the densities of T3, T4, and T5 samples range from 0.85 to 1.00 g/cm^3, and the mass attenuation coefficient (MAC) values obtained for these samples at 662 keV were approximately 0.085 cm^2/g. These results are largely consistent with studies in the literature on wood species with similar densities. For example, Manjunatha (2013), in his study examining the attenuation capacities of wood species with different densities against gamma rays, reported a MAC value of approximately 0.081 cm^2/g at 662 keV for Chloroxylon swietenia, which has a density of 1.186 g/cm^3. In the same study, the MAC value for a lower-density species, Sterculia urens (0.340 g/cm^3), was found to be ~0.080 cm^2/g at a similar energy level, but the HVL and TVL values for this species were reported to be higher. This suggests that species with lower densities exhibit lower attenuation effectiveness despite the same MAC value (Manjunatha, 2013). Similarly, a study by Sayyed et al. (2018) examined the attenuation behavior of various building materials against gamma rays and found that clay briquettes, in particular, with metal oxide additives exhibited lower HVL and TVL values due to increased density. In this study, MAC values were reported for unmixed concrete samples at 662keV in the range of ~0.06–0.08 cm^2/g. These values, while similar when compared to the wood species in our study, indicate that natural wood materials can exhibit similar attenuation performance to unmixed concrete (Sayyed et al., 2018). Furthermore, in a study on building materials used in Turkey by Akkurt et al. (2009), HVL values for some concrete types were measured at 662keV between 2.5 and 4 cm. While these values are lower than the HVL values measured in wood species such as T3, T4, and T5, this difference is understood to be due to the much higher density of concrete (approximately 2.3–2.5 g/cm^3) (Akkurt et al., 2009). These comparisons demonstrate that wood species, as natural and sustainable materials, can be used as effective attenuators against low- and medium-energy gamma rays under certain conditions. In particular, the MAC, HVL, and TVL values of high-density wood species (e.g., T4 and T5) can yield results close to those of some traditional building materials, suggesting that these species could be considered for biomaterial-based radiation protection applications.

4. Result and Discussion

The findings obtained within the scope of this study reveal the attenuation performances of selected wood species against gamma radiation at different energy levels (662 keV, 1173 keV, and 1332 keV) and demonstrate that these

performances are consistently confirmed both experimentally and theoretically. Notably, a strong linear correlation (R^2 = 0.9195) was observed between wood density and the linear attenuation coefficient (LAC) at 662 keV, indicating that low-energy photons interact more effectively with the internal atomic structure of wood materials. Although the slope increased to 0.0929 at 1173 keV, the strength of the correlation decreased (R^2 = 0.7525), suggesting that high-energy photons interact less with density and penetrate more deeply. At 1332 keV, the slope was the lowest (0.06), with a moderate correlation (R^2 = 0.8848), emphasizing that photon attenuation becomes less density-dependent at higher energies.

When the wood samples were evaluated individually, T3, T4, and T5 emerged as the most effective materials for gamma-ray attenuation, especially at 662 keV, where their MAC values approached 0.085. These species maintained relatively better performance at higher energies as well, with MAC values decreasing moderately to ~0.065 at 1173 keV and ~0.060 at 1332 keV. In contrast, sample T1 consistently exhibited the lowest MAC values and the highest HVL and TVL values across all energy levels, with the HVL reaching approximately 125 mm at 1173 keV, indicating minimal attenuation capacity. This suggests that T1 is structurally unsuitable for gamma radiation shielding, likely due to its low density or unfavorable elemental composition. The experimental MAC results were also compared with theoretical values calculated via the XCOM program, and an excellent agreement was observed (R^2 > 0.98) across all energy levels, which confirms the reliability and consistency of the experimental methodology. In terms of practical applications, the study suggests that T3, T4, and T5 are the most promising candidates for radiation shielding at low to medium gamma energy levels (662 keV and 1173 keV), particularly in environments where lightweight, organic, or biodegradable shielding materials are preferred. However, for high-energy photon environments (e.g., 1332 keV and above), the attenuation capacities of all wood types decreased significantly, indicating the need for either composite enhancement or alternative materials with higher effective atomic numbers and densities. For future studies, it is advisable to broaden the scope of investigation to include a wider spectrum of photon energies, particularly by examining both lower diagnostic energy ranges (below 200 keV) and higher therapeutic or industrial energy levels (above 1500 keV). Additionally, integrating heavy metal oxides or nanoparticle additives into wooden matrices could lead to the development of novel bio-composite materials with enhanced radiation shielding properties. Comparative evaluations with conventional shielding materials such as lead, concrete, and polymer-based composites would also provide insight into the cost-effectiveness and practical viability of wood-based alternatives. Moreover, to fully assess their real-world applicability, future research should consider the long-term performance of these materials, focusing on their mechanical stability, environmental resistance, and durability under sustained radiation exposure.

Conflict of Interest

No conflict of interest was declared by the authors.

References

Abouhaswa, A.S., 2019. Synthesis, structure, optical and gamma radiation shielding properties of B2O3-PbO2-Bi2O3 glasses. Compos. B Eng. 172, 218–225.

Agar, O., 2019. An extensive investigation on gamma ray shielding features of Pd/ Ag-based alloys. Nucl. Eng. Technol. 51 (3), 853–859.

Akiyama, H., 1989. 1/10th scale model test of inner concrete structure composed of concrete filled steel bearing wall. In: Transactions of the 10th International Conference on Structural Mechanics in Reactor Technology.

Akkurt, I., Kilincarslan, S., Basyigit, C. (2009). The attenuation of gamma-rays by concretes produced with barite. Progress in Nuclear Energy, 51(1), 91–94. https://doi.org/10.1016/j.pnucene.2008.06.003.

Akkurt, I., Başyiğit, C., Akkaş, A., Kılınçarslan, Ş., Mavi, B., Günoğlu, K., 2012. Determination of some heavyweight aggregate half value layer thickness used for radiation shielding. Acta Physica Polonica A, 121(1), 138-140.

Akkurt, I., Başyigit, C., Kilincarslan, S., Beycioglu, A. 2010. Prediction of photon attenuation coefficients of heavy concrete by fuzzy logic. Journal of the Franklin Institute, 347(9), 1589-1597.

Akkurt, I., Emikönel, S., Akarslan, F., Günoğlu, K., Kilinçarslan, Ş., Üncü, I. 2015. Barite effect on radiation shielding properties of cotton-polyester fabric. Acta Physica Polonica A, 128(2B).

Al-Buriahi, M.S., Rammah, Y.S., 2019. Investigation of the physical properties and gamma-ray shielding capability of borate glasses containing PbO, Al 2 O 3 and Na_2O. Appl. Phys. A 125 (10), 1–8.

Al-Buriahi, M.S., Rammah, Y.S., 2019. Electronic polarizability, dielectric, and gamma- ray shielding properties of some tellurite-based glasses. Appl. Phys. A 125 (10), 1–9.

Al-Buriahi, M.S., Tonguc, B.T., 2020. Mass attenuation coefficients, effective atomic numbers and electron densities of some contrast agents for computed tomography. Radiat. Phys. Chem. 166 (August 2019), 108507 https://doi.org/10.1016/j.radphyschem.2019.108507.

Al-Hadeethi, Y., Sayyed, M.I., 2020. X-ray attenuation features of some tellurite glasses evaluated at medical diagnostic energies. Appl. Math. Comput. 365, 124712.

Almatari, M., et al., 2019. Photon and neutron shielding characteristics of samarium doped lead alumino borate glasses containing barium, lithium and zinc oxides determined at medical diagnostic energies. Res. Phys. 12, 2123–2128.

Bootjomchai, C., et al., 2012. Gamma-ray shielding and structural properties of barium–bismuth–borosilicate glasses. Radiat.

Phys. Chem. 81 (7), 785–790.
Cherkashina, N.I., Pavlenko, A.V.2018. Synthesis of polymer composite based on polyimide and Bi12SiO20 sillenite. Polym. Plast. Technol. Eng. 57 (18), 1923–1931.
Cherkashina, N.I., Pavlenko, V.I., Noskov, A.V.2019. Synthesis and property evaluations of highly filled polyimide composites under thermal cycling conditions from − 190 ◦C to +200 ◦C. Cryogenics 104, 102995. https://doi.org/10.1016/j.cryogenics.2019.102995.
D'Auria, F., Debrecin, N., Glaeser, H., 2017. Strengthening nuclear reactor safety and analysis. Nucl. Eng. Des. 324, 209–219.
El-Khayatt, A.M., Ali, A.M., Singh, V.P., 2014. Photon attenuation coefficients of Heavy-Metal Oxide glasses by MCNP code, XCOM program and experimental data: a comparison study. Nucl. Instrum. Methods Phys. Res. Sect. A Accel. Spectrom. Detect. Assoc. Equip. 735, 207–212. https://doi.org/10.1016/j.nima.2013.09.027.
Ersundu, M.Ç., et al., 2019. Physical, mechanical and gamma-ray shielding properties of highly transparent ZnO-MoO3-TeO2 glasses. J. Non-Cryst. Solids 524, 119648.
Kaewjaeng, S., et al., 2012. Effect of BaO on optical, physical and radiation shielding properties of SiO2-B2O3-Al2O3-CaO-Na2O glasses system. Procedia Eng. 32, 1080–1086.
Kumar, A., et al., 2020. Experimental studies and Monte Carlo simulations on gamma ray shielding competence of (30+ x) PbO10WO3 10Na2O– 10MgO–(40-x) B2O3 glasses. Prog. Nucl. Energy 119, 103047.
Kurudirek, M., 2017. Heavy metal borate glasses: potential use for radiation shielding. J. Alloys Compd. 727, 1227–1236.
Mahmoud, K.A., et al., 2019. Investigation of radiation shielding properties for some building materials reinforced by basalt powder. In: AIP Conference Proceedings. AIP Publishing LLC, 20036.
Mahmoud, K.M., Rammah, Y.S., 2020. Investigation of gamma-ray shielding capability of glasses doped with Y, Gd, Nd, Pr and Dy rare earth using MCNP-5 code. Phys. B Condens. Matter 577, 411756.
Mann, K.S., Sidhu, G.S., 2012. Verification of some low-Z silicates as gamma-ray shielding materials. Ann. Nucl. Energy 40 (1), 241–252.
Manjunatha, H. C. (2013). A study on photon attenuation coefficients of different wood materials with different densities. Annals of Nuclear Energy, 62, 48–53. https://doi.org/10.1016/j.anucene.2013.07.019.
Mettler, F.A., 2012. Medical effects and risks of exposure to ionising radiation. J. Radiol. Prot. 32 (1), N9.
Rachniyom, W., et al., 2018. Effect of Bi2O3 on radiation shielding properties of glasses from coal fly ash. Mater. Today: Proc. 5 (6), 14046–14051.
Sadetzki, S., Mandelzweig, L., 2009. Childhood exposure to external ionising radiation and solid cancer risk. Br. J. Cancer 100 (7), 1021–1025.
Sayyed, M. I., Khandaker, M. U., Ali, M. A. B., & Bradley, D. A. (2018). Radiation shielding characteristics of clay materials with added iron slag for gamma radiation at 662 keV. Results in Physics, 9, 206–211. https://doi.org/10.1016/j.rinp.2018.01.034.
Sayyed, M.I., et al., 2018. Comparative study of gamma-ray shielding and elastic properties of BaO–Bi2O3–B2O3 and ZnO–Bi2O3–B2O3 glass systems. Mater. Chem. Phys. 217, 11–22.
Sayyed, M.I., et al., 2020. Evaluation of gamma-ray and neutron shielding features of heavy metals doped Bi2O3-BaO-Na2O-MgO-B2O3 glass systems. Prog. Nucl. Energy 118, 103118.
Shams, T., Eftekhar, M., Shirani, A., 2018. Investigation of gamma radiation attenuation in heavy concrete shields containing hematite and barite aggregates in multi-layered and mixed forms. Construct. Build. Mater. 182, 35–42.
Shamshad, L., et al., 2017. A comparative study of gadolinium based oxide and oxyfluoride glasses as low energy radiation shielding materials. Prog. Nucl. Energy 97, 53–59.
Sharma, A., et al., 2019. Simulation of shielding parameters for TeO2-WO3-GeO2 glasses using FLUKA code. Res. Phys. 13, 102199.
Sharma, R., et al., 2012. Effective atomic numbers for some calcium–strontium-borate glasses. Ann. Nucl. Energy 45, 144–149.
Shavers, M.R., et al., 2004. Implementation of ALARA radiation protection on the ISS through polyethylene shielding augmentation of the Service Module Crew Quarters. Adv. Space Res. 34 (6), 1333–1337.
Singh, K.J., et al., 2008. Gamma-ray shielding and structural properties of PbO–SiO2 glasses. Nucl. Instrum. Methods Phys. Res. Sect. B Beam Interact. Mater. Atoms 266 (6), 944–948.
Singh, V.P., Badiger, N.M., 2014. Energy absorption buildup factors, exposure buildup factors and Kerma for optically stimulated luminescence materials and their tissue equivalence for radiation dosimetry. Radiat. Phys. Chem. 104, 61–67.
Sodhi, K.S., et al., 2015. Clinical application of 'Justification'and 'Optimization'principle of ALARA in pediatric CT imaging:"How many children can be protected from unnecessary radiation? Eur. J. Radiol. 84 (9), 1752–1757.
Vano, E., 2011. Global view on radiation protection in medicine. Radiat. Protect. Dosim. 147 (1–2), 3–7.
Waly, E.-S.A., Bourham, M.A., 2015. Comparative study of different concrete composition as gamma-ray shielding materials. Ann. Nucl. Energy 85, 306–310.
Waly, E.-S.A., Fusco, M.A., Bourham, M.A., 2016. Gamma-ray mass attenuation coefficient and half value layer factor of some oxide glass shielding materials. Ann. Nucl. Energy 96, 26–30.